

Ischemia-induced neurogenesis of neocortical layer 1 progenitor cells

Koji Ohira^{1–4}, Takahiro Furuta², Hiroyuki Hioki², Kouichi C Nakamura^{2,4,8}, Eriko Kuramoto², Yasuyo Tanaka², Nobuo Funatsu³, Keiko Shimizu⁵, Takao Oishi⁵, Motoharu Hayashi⁵, Tsuyoshi Miyakawa^{1,4,6}, Takeshi Kaneko^{2,4} & Shun Nakamura^{3,4,7}

Adult mammalian neurogenesis occurs in the hippocampus and the olfactory bulb, whereas neocortical adult neurogenesis remains controversial. Several occurrences of neocortical adult neurogenesis in injured neocortex were recently reported, suggesting that neural stem cells (NSCs) or neuronal progenitor cells (NPCs) that can be activated by injury are maintained in the adult brain. However, it is not clear whether or where neocortical NSCs/NPCs exist in the brain. We found NPCs in the neocortical layer 1 of adult rats and observed that their proliferation was highly activated by global forebrain ischemia. Using retrovirus-mediated labeling of layer 1 proliferating cells with membrane-targeted green fluorescent protein, we found that the newly generated neurons were GABAergic and that the neurons were functionally integrated into the neuronal circuitry. Our results suggest that layer 1 NPCs are a source of adult neurogenesis under ischemic conditions.

Neurogenesis in the CNS of adult mammals has been of particular interest to the field of neuroscience for over 100 years¹. New technologies for detecting cell proliferation, such as [³H]-thymidine, 5-bromo-2'-deoxy-uridine (BrdU), immunohistochemistry of chemical markers for proliferating cells and various cell types, retrovirus-mediated cell labeling, and genetically modified animals² have identified adult mammalian neurogenesis in two regions, namely granule and periglomerular neurons in the olfactory bulb from the anterior subventricular zone (aSVZ) and granule cells in the hippocampal dentate gyrus from the subgranular zone (SGZ)³. In addition, a variety of factors can modulate neurogenesis in these regions, including exercise, environmental enrichment, pregnancy and stroke upregulate neurogenesis, whereas stress and aging downregulate it⁴.

Whether adult neocortical neurogenesis occurs or not is highly controversial^{5–13}. This controversy may be a result of the experimental methods and animals' conditions, such as housing condition, animals' histories, and genetic background and technical problems⁴. Recent studies have reported generation of new neurons in the adult mammalian neocortex under pathologic conditions^{14–22}, suggesting that NSCs or NPCs that can be upregulated by brain injury and stroke may be maintained in the neocortex. Using combined immunohistochemistry and retroviral labeling method, we found NPCs in the neocortical layer 1 of the adult rats. Furthermore, we found that the layer 1 NPCs produced GABAergic interneurons under ischemic conditions.

RESULTS

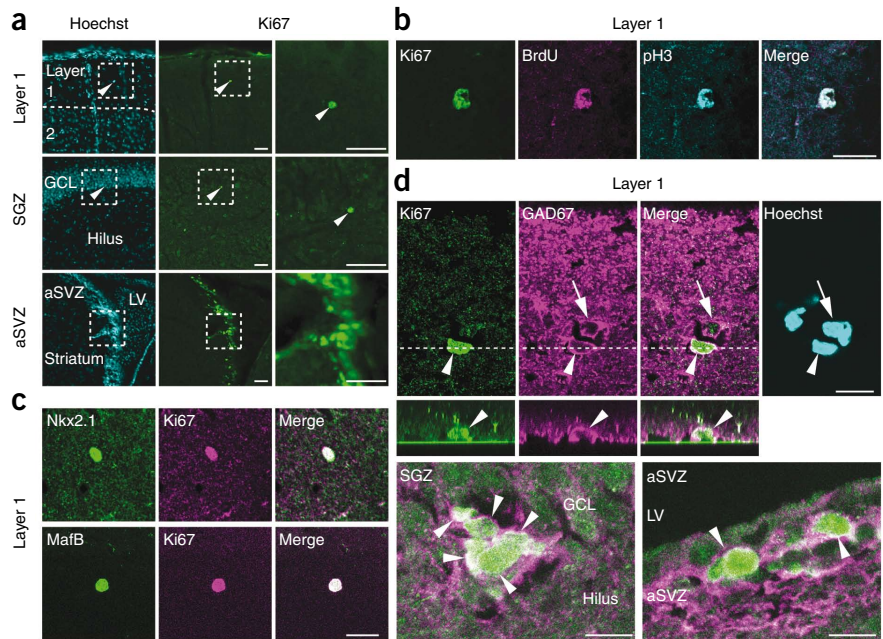
Proliferating cells in the neocortical layer 1

To identify proliferating cells in and beneath the neocortex of adult rats, we used the cell proliferation marker Ki67, which is expressed in cell nuclei during all of the phases of the cell cycle, except for G₀. Immunohistochemical analysis revealed that Ki67-positive cells were distributed in layer 1, as well as in the SGZ and aSVZ (**Fig. 1a**). In addition, we found that two other cell proliferation markers, phosphorylated histone H3 (pH3), which is phosphorylated in the M phase, and BrdU, which is incorporated into the newly synthesized DNA during the S phase, were present in layer 1 Ki67-positive cells (**Fig. 1b**). Furthermore, almost all of the layer 1 Ki67-positive cells were lacked the NSC marker nestin, the neuronal markers TuJ1, NeuN and calretinin, the astrocyte marker S100, the oligodendrocyte marker proteolipid protein, the microglia marker CD11b, and the vascular and endothelial progenitor cell marker CD34 (**Supplementary Fig. 1**).

Although layer 1 Ki67-positive cells were lacked the neuronal markers TuJ1, NeuN and calretinin, glutamic acid decarboxylase 67 (GAD67) was produced in 668 of 933 layer 1 Ki67-positive cells (mean \pm s.d., 70.3 \pm 23.6%, n = 7 rats; **Fig. 1**). As NSCs/NPCs in the SGZ and aSVZ express GAD67 (refs. 23,24) (**Fig. 1**), this finding suggests that layer 1 Ki67 and GAD67 double-positive cells may be proliferating cells. Moreover, Nkx2.1 and MafB, which are molecular markers of cells derived from the ganglionic eminence^{25,26}, were coexpressed in 111 of 147 layer 1 Ki67-positive cells (79.1 \pm 18.8%, n = 5 rats) and

¹Division of Systems Medical Science, Institute for Comprehensive Medical Science, Fujita Health University, Toyoake, Aichi, Japan. ²Department of Morphological Brain Science, Graduate School of Medicine, Kyoto University, Kyoto, Japan. ³Department of Biochemistry and Cellular Biology, National Institute of Neuroscience, National Center of Neurology and Psychiatry, Tokyo, Japan. ⁴Japan Science and Technology Agency (JST), Core Research for Evolutional Science and Technology (CREST), Kawaguchi, Saitama, Japan. ⁵Department of Cellular and Molecular Biology, Primate Research Institute, Kyoto University, Inuyama, Aichi, Japan. ⁶Center for Genetic Analysis of Behavior, National Institute for Physiological Sciences, Myodaiji, Okazaki, Aichi, Japan. ⁷Department of Biotechnology and Life Science, Tokyo University of Agriculture and Technology, Koganei, Tokyo, Japan. ⁸Present address: Medical Research Council Anatomical Neuropharmacology Unit, University of Oxford, Oxford, UK, and Human Frontier Science Program, Strasbourg Cedex, France. Correspondence should be addressed to K.O. (ohira@fujita-hu.ac.jp) or T.K. (kaneko@mbs.med.kyoto-u.ac.jp).

Figure 1 Characterization of layer 1 proliferating cells. **(a)** Ki67 expression in layer 1, SGZ and aSVZ. Right, higher magnification of the boxed areas in the middle column. Arrowheads indicate the same cells in each row. Scale bars represent 40 μm . **(b)** Layer 1 Ki67-positive cells contained other proliferating cell markers, BrdU and pH3. Scale bar represents 20 μm . **(c)** Layer 1 Ki67-positive cells expressed the ganglionic eminence markers Nkx2.1 and MafB. Scale bar represents 20 μm . **(d)** Ki67-positive cells in layer 1, SGZ and aSVZ expressed GAD67. The arrowheads indicate Ki67 and GAD67 double-positive proliferating cells in layer 1, SGZ and aSVZ. The arrow indicates Ki67-negative, GAD67-positive interneuron in the layer 1. GCL, granule cell layer; LV, lateral ventricle. Scale bars represent 10 μm .



in 122 of 162 layer 1 Ki67-positive cells ($81.2 \pm 22.8\%$, $n = 5$ rats), respectively (**Fig. 1c**). These results suggest that layer 1 Ki67 and GAD67 double-positive cells might be ganglionic eminence-derived proliferating cells.

We next examined the effect of ischemic treatment on layer 1 Ki67 and GAD67 double-positive proliferating cells. Common carotid arteries of rats were clamped on both sides transiently for 10 min. The ischemic treatment induced an increase in the number of microglia but did not induce increased cell death of NeuN-positive cells at 1 week following ischemic treatment (**Supplementary Fig. 2**), suggesting that the ischemic treatment was not so severe. Although the number of Ki67-positive cells was markedly increased in all neocortical layers by 1 week after the global ischemic treatment, Ki67 and GAD67 double-positive cells were almost exclusively observed in layer 1 of both sham-operated control and ischemia-treated rats (**Fig. 2a,b**). The number of layer 1 Ki67 and GAD67 double-positive cells in ischemia-treated rats increased 1.56-fold compared with controls ($P < 0.01$, $n = 6$ rats for each time point, two-way ANOVA followed by Tukey's *post hoc* test) at 1 week after ischemia and returned control levels by 2 weeks post treatment (**Fig. 2b**). Similar transient increase of Nkx2.1 and Ki67 double-positive cells was observed (**Supplementary Fig. 3**). Layer 1

Ki67 and GAD67 double-positive cells were ubiquitously distributed in layer 1 of the frontal, motor, somatosensory and visual cortices under both the control and ischemic conditions (**Fig. 2c**). Other Ki67-positive, GAD67-negative cells (**Fig. 2a**), at least some of them, might be proliferating cells for reactive gliosis, such as NG2-positive and Olig2-positive proliferating cells, induced by ischemic treatment (**Supplementary Fig. 4**).

Generation of GABAergic neurons under ischemic condition

Our results indicate that proliferating cells exist in layer 1 of the adult rat neocortex. We next sought to determine whether layer 1 proliferating cells produce neurons, neuroglia or both cell species. To trace the morphological and chemical details and migration of newly generated cells from layer 1 proliferating cells, we used a recombinant retrovirus vector expressing membrane-targeted GFP under the cytomegalovirus (CMV) promoter²⁷ (only proliferating cells incorporate the

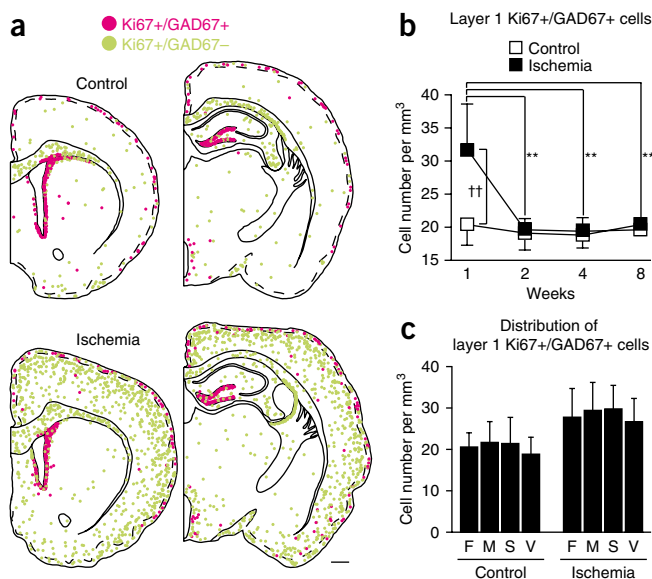
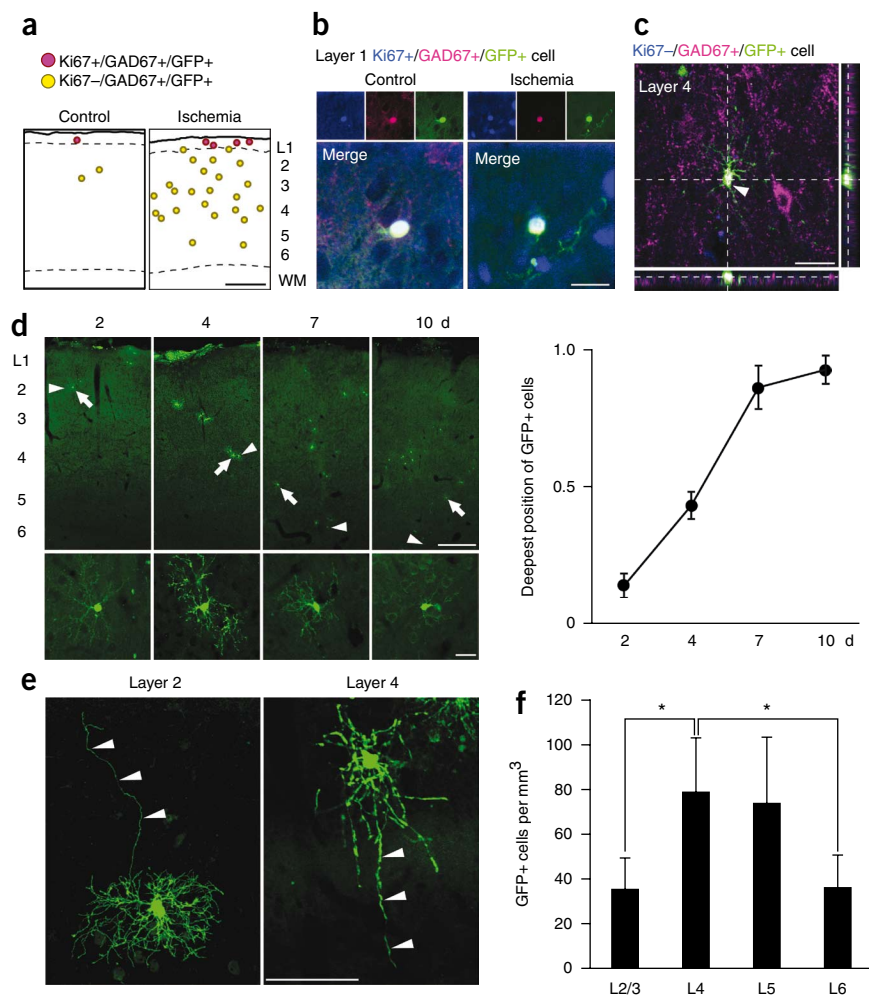


Figure 2 Distribution of layer 1 proliferating cells in the control and ischemic brains. **(a)** Distribution of Ki67 and GAD67 double-positive cells in control and ischemia-treated brains of adult rats. Representative drawings through the neostriatum (left) and thalamic nuclei (right) are shown in each row. The labeled somata of ten serial 50- μm -thick sections were superimposed to create the images. Scale bar represents 1 mm. **(b)** Time course quantification of layer 1 Ki67 and GAD67 double-positive cells after ischemic treatment. ** indicates significant difference between the value at 1 week and at other weeks; †† indicates significant differences between ischemia-treated and control brains ($P < 0.01$, two-way ANOVA followed by Tukey's *post hoc* test, $n = 3$ rats for each time and condition). Data are shown as mean \pm s.d. **(c)** Distribution of layer 1 Ki67 and GAD67 double-positive cells in the frontal (F), motor (M), somatosensory (S) and visual (V) cortices 1 week after ischemic treatment. There were no difference in the distribution of layer 1 Ki67 and GAD67 double-positive cells among the F, M, S and V cortices in control and ischemic conditions ($P = 0.43$ and 0.75 , two-way ANOVA for control and ischemic conditions, respectively, $n = 3$ rats), although there was a significant difference in each cortical region by comparing control versus ischemic treatment (all regions, $P < 0.05$, two-sided *t* test, $n = 3$ rats). Data are shown as mean \pm s.d.

Figure 3 Retrovirus-mediated GFP labeling of layer 1 proliferating cells. **(a)** Distribution of Ki67, GAD67 and GFP triple-positive and Ki67-negative, GAD67-positive, GFP-positive cells in the somatosensory cortex 4 weeks after ischemia. The labeled somata of five serial 50- μm -thick sections were superimposed in a drawing. WM, white matter. Scale bar represents 500 μm . **(b)** Layer 1 proliferating cells labeled with antibodies to Ki67, GAD67 and GFP 1 week after ischemia. Scale bar represents 20 μm . **(c)** A layer 4 postmitotic cell labeled with antibodies to Ki67, GAD67 and GFP 1 week after ischemic treatment (arrowhead). Scale bar represents 30 μm . **(d)** Time course of the positional changes of GFP-positive cells in layer 2–6 after ischemia. Higher magnifications of cells indicated by the arrows are shown below. Arrowheads indicate the deepest positioned GFP-positive cells. The deepest positions of GFP-positive cells were plotted against days post ischemia. The positions were expressed by a relative value between the cortical surface (0) and the border with the white matter (1). Scale bars represent 300 μm (top) and 30 μm (bottom). **(e)** Layer 2 and layer 4 GFP-positive cells in the somatosensory cortex 4 weeks after ischemia. Arrowheads indicate an axon-like process. **(f)** Laminal distribution of GFP-positive cells 4 weeks after ischemia (* $P < 0.05$, two-way ANOVA followed by Tukey's *post hoc* test, $n = 4$ rats). All data are shown as means \pm s.d. Scale bar represents 50 μm .



transgene into their genome) and visualized the detailed cell morphology of daughter cells from layer 1 proliferating cells.

We injected the recombinant retrovirus vectors into layer 1 and confirmed that the injected solution was largely confined to layer 1 using sham injections of the nuclear dye Hoechst 33258 (**Supplementary Fig. 5**). Ki67, GAD67 and GFP triple-positive cells were found only in or just beneath layer 1 (**Fig. 3a**) and possessed a round cell body with a few short processes (**Fig. 3b**). The morphology of layer 1 Ki67, GAD67 and GFP triple-positive cells was not substantially changed by the ischemic treatment (**Fig. 3b**). In contrast, the ischemic treatment produced a large increase in the number of Ki67-negative, GAD67-positive and GFP-positive cells in layer 2–6 (**Fig. 3a,c**). Thus, we assumed that GFP-positive cells would have become postmitotic and migrated from layer 1 to deep layers.

To address the migration of GFP-positive cells from layer 1, we observed the time course of the distribution of GFP-positive cells after ischemia. GFP-positive cells were found mostly in layer 2–3 at 2 d, in layer 2–4 at 4 d and in layer 2–6 at 7 and 10 d post ischemia, namely the deepest position fell with the day after ischemia (**Fig. 3d**). These findings suggest that Ki67-negative, GAD67-positive, GFP-positive cells, which were produced from layer 1 Ki67, GAD67 and GFP triple-positive cells by the ischemic stimuli, migrated to the deepest layers within 7–10 d of the ischemia treatment.

Notably, the morphology of newly generated GFP-positive cells was almost uniform and similar to that of neurons, which had round cell bodies, radially extending dendrite-like processes and longer axon-like processes (**Fig. 3e**). They were distributed in all cortical layers 1–8 weeks after ischemia and were most frequently found in layer 4 ($P < 0.05$, $n = 4$ rats, two-way ANOVA followed by Tukey's *post hoc* test; **Fig. 3f**). It is noteworthy that at 4 weeks after ischemia, immature and mature neuronal markers, TuJ1, HuC/D and MAP2, were expressed

in 34 of 77 layer 2–6 GFP-positive cells ($46.0 \pm 15.6\%$, $n = 3$ rats), in 49 of 76 GFP-positive cells ($64.4 \pm 4.19\%$, $n = 3$ rats) and in 77 of 98 GFP-positive cells ($77.8 \pm 13.6\%$, $n = 3$ rats), respectively (**Fig. 4a**). In addition, we found that a large number of the GFP-positive cells expressed voltage-gated sodium channels (Na_v), which are essential for the production of action potentials²⁸, using a pan- Na_v antibody and an antibody to $\text{Na}_v1.6$ (86 of 120 GFP-positive cells were pan- Na_v positive: $71.7 \pm 14.4\%$, $n = 3$ rats; 98 of 162 GFP-positive cells were $\text{Na}_v1.6$ positive: $60.0 \pm 11.8\%$, $n = 3$ rats; **Fig. 4b**). However, few layer 2–6 GFP-positive cells were colabeled with glial marker antibodies (antibodies to GFAP were used to label astrocytes, an antibody raised against rat glial membrane and whole-brain white matter was used to label oligodendrocytes, and antibodies to CD11b were used to label microglia) up to 8 weeks after ischemia (**Table 1** and **Supplementary Fig. 6**). These findings suggest that GFP-positive cells in layer 2–6 share the morphological and molecular characteristics of neurons. We confirmed this using a different retrovirus vector, which expressed membrane-targeted GFP under the control of the *SYN1* (synapsin 1) promoter²⁹, a well-known neuron-specific promoter. Using this recombinant retrovirus, we found GFP-positive cells in layer 2–6 4 weeks after the ischemia that were the same type as those that we found using retrovirus with CMV promoter (**Fig. 4a**).

In contrast, few neurons were generated when the retrovirus was injected into the SVZ and white matter, which are the other candidate regions for supplying new neocortical neurons^{15,17,30} (**Supplementary Fig. 6**), except for neurons migrating to the olfactory

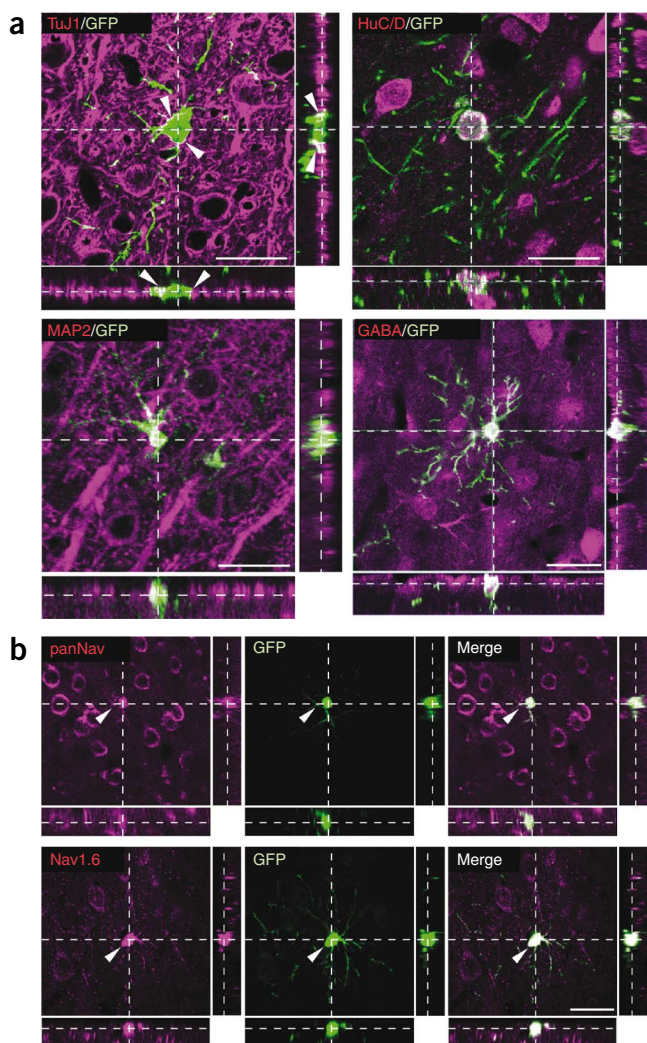


Figure 4 Double-staining of layer 2–6 GFP-positive cells with cell markers. **(a)** Layer 2–6 GFP-positive cells were co-stained with antibodies to neuronal markers (TuJ1, HuC/D and MAP2). Arrowheads indicate TuJ1 and GFP double-positive cell body structures. Bottom right, a layer 3 newly generated cells, which expressed GFP under the control of *SYN1* promoter, was GABA immunoreactive. **(b)** GFP-positive cells expressed voltage-gated sodium channels (top, layer 3, panNav_v; below, layer 2, Nav1.6). All images were taken from the somatosensory cortex 4 weeks after ischemic treatment. Scale bars represent 30 μ m.

analysis of GFP and neuronal subpopulation markers. Each of the markers for GABA, neuropeptide Y (NPY), choline acetyltransferase (ChAT), somatostatin (SOM) and calretinin were expressed in layer 2–6 GFP-positive neurons up to 8 weeks post ischemia (**Fig. 5a** and **Table 1**). The colabeling rates of the markers in GFP-positive neurons increased as time elapsed up to 4 weeks after ischemia (% at 1, 2 and 4 weeks after ischemia, means \pm s.d.; GABA: 42.9 ± 2.15 , 67.5 ± 12.4 , 81.2 ± 6.06 ; NPY: 25.8 ± 6.26 , 34.8 ± 18.9 , 39.7 ± 12.9 ; ChAT: 1.33 ± 0.980 , 2.46 ± 0.811 , 4.61 ± 2.75 ; SOM: 2.01 ± 1.10 , 3.07 ± 1.38 , 10.9 ± 4.00). This implies that the newly generated neurons matured and/or that the newly generated immature neurons died. The calcium-binding proteins calbindin and parvalbumin, each of which is expressed in a subpopulation of GABAergic neurons, were not observed in GFP-positive neurons (**Table 1**). In GABAergic neurons of the rat frontal cortex, NPY and calretinin expression are mutually exclusive³¹. Indeed, summations of the expression rates of NPY and calretinin in new neurons were similar to those of GABA-containing neurons up to 4 weeks after ischemia (**Table 1**). Both the expression of the markers and the number of new neurons at 8 weeks after ischemia might decrease, as new neurons might be short lived.

Recently, multipolar calretinin cells have been shown to coexpress SOM in the mouse³². We examined whether calretinin and GFP double-positive cells contained SOM and found no calretinin, SOM and GFP triple-positive cells (**Fig. 5b**). This result is compatible with the previous report that there are three groups of rat cortical interneurons, each of which expresses parvalbumin, calretinin and SOM in a mutually exclusive manner³¹.

bulb (**Supplementary Fig. 6**). In contrast, astrocytes and oligodendrocytes were labeled mainly in the SVZ, white matter and occasionally in layer 6 (**Supplementary Fig. 6**). This result indicates that new neocortical neurons may not be generated in the SVZ or white matter in these conditions.

We further examined the chemical properties of layer 2–6 GFP-positive neurons in ischemia-treated rats, using double-staining

Time course analysis of new neurons after ischemia

To reduce experimental error in the quantitative time course analysis of neuronal production after ischemia, we injected the retrovirus solution into as many sites as possible in layer 1 of the somatosensory neocortex of a rat (see Online Methods). In addition, we serially sectioned a whole brain from the olfactory bulb to the posterior region of midbrain, stained all of the resulting sections with antibody

Table 1 Phenotypes of GFP-positive postmitotic cells

	Periods after ischemic treatment			
	1 week	2 weeks	4 weeks	8 weeks
<i>n</i> (rats)	3	3	3	3
GABA	42.9 ± 2.15 (133)	$67.5 \pm 12.4^*$ (91)	$81.2 \pm 6.06^{\#}$ (84)	$80.3 \pm 7.54^{\#}$ (30)
NPY	25.8 ± 6.26 (162)	34.8 ± 18.9 (40)	39.7 ± 12.9 (63)	30.6 ± 12.7 (24)
ChAT	1.33 ± 0.980 (112)	2.46 ± 0.811 (68)	4.61 ± 2.75 (51)	4.58 ± 2.20 (29)
SOM	2.01 ± 1.10 (124)	3.07 ± 1.38 (75)	$10.9 \pm 4.00^*$ (73)	$9.84 \pm 3.89^*$ (34)
CR	19.2 ± 11.5 (170)	30.5 ± 16.9 (29)	36.7 ± 12.0 (66)	18.6 ± 3.42 (33)
CB	n.d. (272)	n.d. (38)	n.d. (61)	n.d. (25)
PV	n.d. (187)	n.d. (39)	n.d. (93)	n.d. (25)
GFAP	n.d. (226)	n.d. (69)	n.d. (81)	n.d. (21)
Oligodendrocytes	n.d. (162)	n.d. (45)	n.d. (49)	n.d. (23)
CD11b	n.d. (165)	n.d. (78)	n.d. (82)	n.d. (31)

Data are presented as mean \pm s.d. from three rats at each time point. The total numbers of counted cells are shown in parentheses. One-way ANOVA and Tukey's *post hoc* test was used in the statistic analysis of time course of each marker. * $P < 0.05$, $^{\#}P < 0.01$, significant difference compared with each value of 1 week. n.d., not detectable. CB, calbindin; CR, calretinin; PV, parvalbumin.

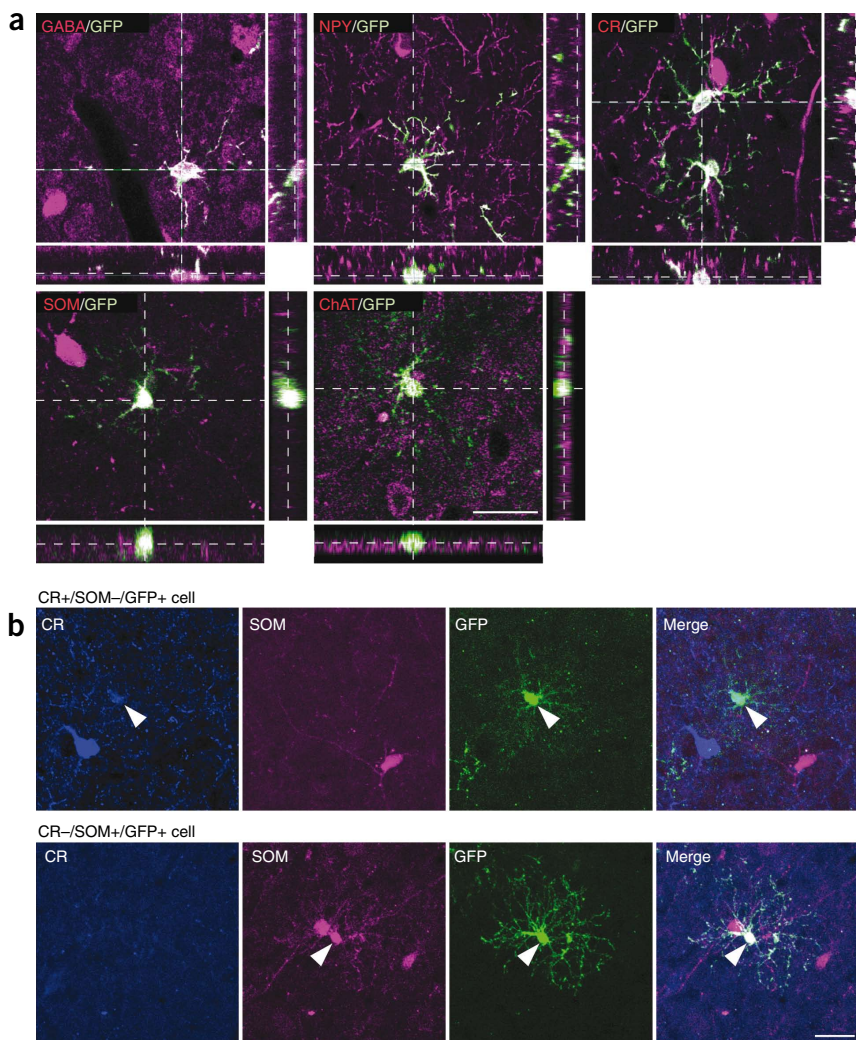


Figure 5 Characterization of layer 2–6 GFP-positive cells with neurochemical markers. (a) Layer 2–6 GFP-positive cells were co-stained with antibodies to the molecular markers (magenta) GABA, NPY, calretinin (CR), SOM and ChAT. (b) Triple labeling with calretinin (blue), SOM (magenta) and GFP (green) in newly generated cells. Coexpression of calretinin and SOM in layer 2–6 GFP-positive cells was rarely observed, consistent with the mutually exclusive expression of calretinin and SOM. Arrowheads point to a calretinin-positive, SOM-negative, GFP-positive cell (top) and a calretinin-negative, SOM-positive, GFP-positive cell (bottom). All images were taken from the somatosensory cortex 4 weeks after ischemia. Scale bars represent 30 μm .

expressed in response to various physiological stimuli, including the exposure of animals to a new enriched environment^{34–37}. We examined c-Fos expression in GFP-positive neurons 4 weeks after ischemic treatment, which were generated by the retrovirus injection and ischemic treatment, in response to the exposure to the enriched environment (Fig. 7a). As the whisker system is known to be very active when the rat is exploring a new enriched environment, we examined c-Fos expression in GFP-positive cells in the barrel cortex of the primary somatosensory cortex. When the rats were housed in the original cage, a very few GFP-positive neurons showed c-Fos immunoreactivity (control; $2.5 \pm 4.1\%$, 1 of 40 GFP-positive neurons, $n = 3$ rats; Fig. 7b). However, 2 h after the exposure to a new enriched environment (Supplementary Fig. 7), the percentage of GFP-positive neurons

that expressed c-Fos was much higher (enriched; $17.5 \pm 14.2\%$, 6 of 41 GFP-positive neurons, $n = 3$ rats; Fig. 7b). This result suggests that at least some of the newly generated neurons were functionally incorporated into the cortical circuit.

Although previous reports have shown that c-Fos is expressed in astrocytes after brain injury, c-Fos expression disappears within

to GFP and counted all of the GFP-positive cells. To correct the variances in retrovirus infection efficiency, we calculated the labeling efficiency r (the number of layer 1 Ki67, GAD67 and GFP triple-positive cells divided by the number of layer 1 Ki67 and GAD67 double-positive cells; Supplementary Table 1) and determined the estimated numbers (the number of layer 2–6 GFP-positive neurons) divided by r of newly generated layer 2–6 neurons for each rat.

In the control rats, a small number of layer 2–6 GFP-positive neurons were produced up to 8 weeks after injection of the virus solution (Fig. 6). However, this small number of GFP-positive neurons might be overestimated, as brain damage resulting from virus injection would enhance the proliferation of layer 1 Ki67 and GAD67 double-positive cells. In contrast, at 1 week post ischemia, the number of layer 2–6 GFP-positive neurons was 28-fold larger than that in the sham-operated control rats ($P < 0.01$, $n = 5$ rats, two-way ANOVA followed by Tukey's *post hoc* test), corresponding to 0.93% and 3.7% of total neurons and GABAergic ones in the adult rat neocortex³³, respectively. The number of GFP-positive neurons declined substantially (>70%) by 2 weeks after ischemia.

Integration of new neurons into the neuronal circuitry

Finally, we addressed the question of whether or not these newly generated neurons were functionally integrated into the neuronal circuitry. c-Fos, an immediate early gene product, is known to be

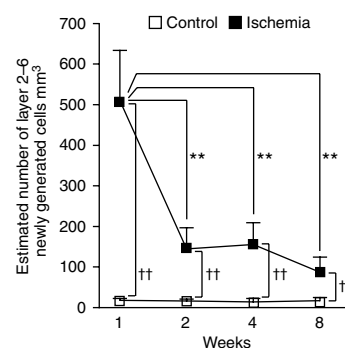


Figure 6 Time course of the estimated number of layer 2–6 GFP-positive cells after ischemia. ** indicates significant difference between the value at 1 week and at other weeks; †† indicates significant differences between ischemia-treated and control brains ($P < 0.01$; two-way ANOVA followed by Tukey's *post hoc* test, $n = 5–6$ rats for each time and condition). Data are shown as mean \pm s.d.

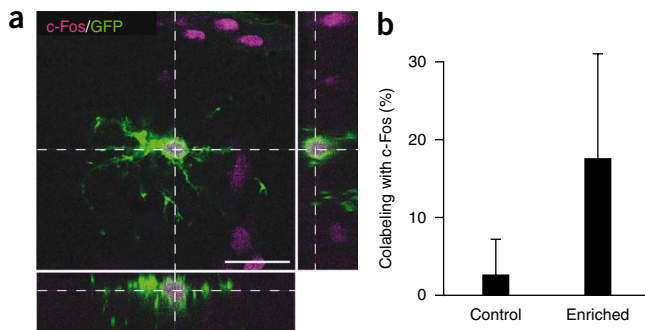


Figure 7 Integration of new neurons into the neuronal circuitry after ischemia. **(a)** A GFP and c-Fos double-positive cell in the layer 2/3 of somatosensory cortex of ischemia-treated rats after exposure to a new enriched environment at 4 weeks after ischemic treatment. Scale bar represents 20 μ m. **(b)** Quantification of c-Fos immunoreactivity in layer 2–6 GFP-positive neurons. c-Fos was expressed more frequently in rats exposed to a new enriched environment than in the control rats (mean \pm s.d., $P < 0.01$, two-sided t test, $n = 3$ rats).

several days^{38,39}. In fact, we found that almost all c-Fos expression was confined to neurons 4 weeks after ischemia (**Supplementary Fig. 7**).

DISCUSSION

We found NPCs in layer 1 of adult rat neocortex, which we refer to as layer 1 inhibitory neuron progenitor (L1-INP) cells (**Supplementary Fig. 8**). L1-INP cells were markedly activated to produce GABAergic neurons by mild ischemic treatment. However, we do not exclude the possibility that neocortical neurons are produced from the ischemia-induced NSCs and NPCs in the SVZ, in white matter or in some unknown region. In fact, the aSVZ seems to generate neocortical neurons under pathologic conditions. For example, corticothalamic pyramidal projection neurons in the neocortex of adult mice are newly generated in layer VI from the aSVZ NPCs when apoptosis of pyramidal projection neurons is induced by chromophore-targeted laser photolysis¹⁵. The focal cerebral ischemia caused by 90-min, 2-h or permanent clump (7–90 d until perfusion), which results in much stronger infarct than is induced in our experiment, causes the generation of new neurons from the aSVZ^{17,21,22}. Furthermore, aspiration lesion of the cortex induces the migration of neuroblasts from the aSVZ to cortical lesion sites¹⁸. However, when we injected retrovirus vectors into the SVZ and white matter before mild ischemic treatment (**Supplementary Fig. 6**), we found few newly generated neurons, indicating that almost all of the newly generated neurons were derived from L1-INP cells, at least under the present conditions of mild ischemic treatment. Thus, damage-induced neurogenesis might be different in its origin depending on the degree and the kind of brain damage.

Although the neocortex is composed of neurons of diverse origins, such as neuroepithelium, the olfactory primordium and ganglionic eminence^{40–42}, almost all cortical GABAergic neurons and their stem cells are developmentally derived from the ganglionic eminence^{43,44}. Because the L1-INP cells expressed some ganglionic eminence markers, such as Nkx2.1 and MafB, L1-INP cells may be of ganglionic eminence origin and maintained in layer 1 of the adult cortex.

What functions do newly generated neurons have? One possibility is hinted at by the fact that the newly generated neurons contained GABA, NPY and SOM (**Fig. 5** and **Table 1**). Convulsion and epilepsy are known to often occur after brain damage, such as ischemic and traumatic injuries⁴⁵. Recent studies have reported that NPY and SOM

have anti-convulsant and anti-epileptogenic functions, suppressing neuronal activity^{46,47}. Thus, newly generated neurons might protect the brain from damage, suppressing abnormal neuronal activities by the anti-convulsant and anti-epileptogenic effects of NPY and SOM, as well as their GABAergic inhibitory actions. If we can regulate the proliferation of L1-INP cells and the survival and differentiation of new neurons in the future, then these cells will be clinically useful for the treatment of convulsion and epilepsy associated with brain damage.

METHODS

Methods and any associated references are available in the online version of the paper at <http://www.nature.com/natureneuroscience/>.

Note: Supplementary information is available on the Nature Neuroscience website.

ACKNOWLEDGMENTS

We would like to thank T.J. Hope for a kindly gift of WPRE, and K. Takumi, M. Itoh, T. Kunieda and H. Kameda for their experimental support. This work was supported by Grants-in-Aid from the Ministry of Education, Culture, Sports, Science and Technology (K.O., T.F., H.H., K.C.N., T.M., T.K. and S.N.) and the Organization for Pharmaceutical Safety and Research (S.N.), by the Cooperation Research Program of Primate Research Institute of Kyoto University (K.O.) and by the Core Research for Evolutional Science and Technology of Japan Science and Technology Agency (K.O., K.C.N., T.M., T.K. and S.N.).

AUTHOR CONTRIBUTIONS

K.O. designed and performed most of the experiments and co-wrote the paper. T.F. and H.H. made the pBS-CMV-Fyn-GFP-WPRE and pENT-Synapsin I-Fyn-GFP-WPRE plasmids. K.C.N. made guinea pig and rabbit antibodies to GFP. E.K., Y.T., N.F., K.S., T.O., M.H. and T.M. supported the experiments. T.K. and S.N. co-wrote the paper. All authors discussed the results and commented on the manuscript.

Published online at <http://www.nature.com/natureneuroscience/>.

Reprints and permissions information is available online at <http://www.nature.com/reprintsandpermissions/>.

- Gross, C.G. Neurogenesis in the adult brain: death of a dogma. *Nat. Rev. Neurosci.* **1**, 67–73 (2000).
- Ming, G.L. & Song, H. Adult neurogenesis in the mammalian central nervous system. *Annu. Rev. Neurosci.* **28**, 223–250 (2005).
- Gage, F.H. Mammalian neural stem cell. *Science* **287**, 1433–1438 (2000).
- Abrous, D.N., Koehl, M. & Le Moal, M. Adult neurogenesis: from precursors to network and physiology. *Physiol. Rev.* **85**, 523–569 (2005).
- Altman, J. Autoradiographic investigation of cell proliferation in the brains of rats and cats. *Anat. Rec.* **145**, 573–591 (1963).
- Kaplan, M.S. Neurogenesis in the 3-month-old rat visual cortex. *J. Comp. Neurol.* **195**, 323–338 (1981).
- Gould, E., Reeves, A.J., Graziano, M.S.A. & Gross, C.G. Neurogenesis in the neocortex of adult primates. *Science* **286**, 548–552 (1999).
- Kornack, D.R. & Rakic, P. Cell proliferation without neurogenesis in adult primate neocortex. *Science* **294**, 2127–2130 (2001).
- Bernier, P.J., Bédard, A., Vinet, J., Lévesque, M. & Parent, A. Newly generated neurons in the amygdala and adjoining cortex of adult primates. *Proc. Natl. Acad. Sci. USA* **99**, 11464–11469 (2002).
- Koketsu, D., Mikami, A., Miyamoto, Y. & Hisatsune, T. Nonrenewal of neurons in the cerebral neocortex of adult macaque monkeys. *J. Neurosci.* **23**, 937–942 (2003).
- Ehninger, D. & Kempermann, G. Regional effects of wheel running and environmental enrichment on cell genesis and migration proliferation in the adult murine neocortex. *Cereb. Cortex* **13**, 845–851 (2003).
- Dayer, A.G., Cleaver, K.M., Abouantoun, T. & Cameron, H.A. New GABAergic interneurons in the adult neocortex and striatum are generated from different precursors. *J. Cell Biol.* **168**, 415–427 (2005).
- Spalding, K.L., Bhardwaj, R.D., Buchholz, B.A., Druid, H. & Frisén, J. Retrospective birth dating of cells in humans. *Cell* **122**, 133–143 (2005).
- Gu, W., Brännström, T. & Wester, P. Cortical neurogenesis in adult rats after reversible photothrombotic stroke. *J. Cereb. Blood Flow Metab.* **20**, 1166–1173 (2000).
- Magavi, S.S., Leavitt, B.R. & Macklis, J.D. Induction of neurogenesis in the neocortex of adult mice. *Nature* **405**, 951–955 (2000).
- Jiang, W. *et al.* Cortical neurogenesis in adult rats after transient middle cerebral artery occlusion. *Stroke* **32**, 1201–1207 (2001).
- Jin, K. *et al.* Directed migration of neuronal precursors into the ischemic cerebral cortex and striatum. *Mol. Cell. Neurosci.* **24**, 171–189 (2003).
- Sundholm-Peters, N.L. *et al.* Subventricular zone neuroblasts emigrate toward cortical lesions. *J. Neuropathol. Exp. Neurol.* **64**, 1089–1100 (2005).

19. Tonchev, A.B., Yamashima, T., Sawamoto, K. & Okano, H. Enhanced proliferation of progenitor cells in the subventricular zone and limited neuronal production in the striatum and neocortex of adult macaque monkeys after global cerebral ischemia. *J. Neurosci. Res.* **81**, 776–788 (2005).
20. Jin, K. *et al.* Evidence for stroke-induced neurogenesis in the human brain. *Proc. Natl. Acad. Sci. USA* **103**, 13198–13202 (2006).
21. Leker, R.R. *et al.* Long-lasting regeneration after ischemia in the cerebral cortex. *Stroke* **38**, 153–161 (2007).
22. Yang, Z. *et al.* Sustained neocortical neurogenesis after neonatal hypoxic/ischemic injury. *Ann. Neurol.* **61**, 199–208 (2007).
23. Stewart, R.R., Hogo, G.J., Zigova, T. & Luskin, M.B. Neural progenitor cells of the neonatal rat anterior subventricular zone express functional GABA_A receptors. *J. Neurobiol.* **50**, 305–322 (2002).
24. Tozuka, Y., Fukuda, S., Namba, T., Seki, T. & Hisatsune, T. GABAergic excitation promotes neuronal differentiation in adult hippocampal progenitor cells. *Neuron* **47**, 803–815 (2005).
25. Cobos, I., Long, J.E., Thwin, M.T. & Rubenstein, J.L. Cellular patterns of transcription factor expression in developing cortical interneurons. *Cereb. Cortex* **16**, i82–i88 (2006).
26. Flames, N. *et al.* Delineation of multiple subpallial domains by the combinatorial expression of transcriptional codes. *J. Neurosci.* **27**, 9682–9695 (2007).
27. Kameda, H. *et al.* Targeting green fluorescent protein to dendritic membrane in central neurons. *Neurosci. Res.* **61**, 79–91 (2008).
28. Kress, G.J. & Mennerick, S. Action potential initiation and propagation: upstream influences on neurotransmission. *Neuroscience* **158**, 211–222 (2009).
29. Hioki, H. *et al.* Efficient gene transduction of neurons by lentivirus with enhanced neuron-specific promoters. *Gene Ther.* **14**, 872–882 (2007).
30. Nunes, M.C. *et al.* Identification and isolation of multipotential neural progenitor cells from the subcortical white matter of the adult human brain. *Nat. Med.* **9**, 439–447 (2003).
31. Kubota, Y., Hattori, R. & Yui, Y. Three distinct subpopulations of GABAergic neurons in rat frontal agranular cortex. *Brain Res.* **649**, 159–173 (1994).
32. Xu, X., Roby, K.D. & Callaway, E.M. Mouse cortical inhibitory neuron type that coexpresses somatostatin and calretinin. *J. Comp. Neurol.* **499**, 144–160 (2006).
33. Ren, J.Q., Aika, Y., Heizmann, C.W. & Kosaka, T. Quantitative analysis of neurons and glial cells in the rat somatosensory cortex, with special reference to GABAergic neurons and parvalbumin-containing neurons. *Exp. Brain Res.* **92**, 1–14 (1992).
34. Staiger, J.F. *et al.* Exploration of a novel environment leads to the expression of inducible transcription factors in barrel-related columns. *Neuroscience* **99**, 7–16 (2000).
35. Carlén, M. *et al.* Functional integration of adult-born neurons. *Curr. Biol.* **12**, 606–608 (2002).
36. Kee, N., Teixeira, C.M., Wang, A.H. & Frankland, P.W. Preferential incorporation of adult-generated granule cells into spatial memory networks in the dentate gyrus. *Nat. Neurosci.* **10**, 355–362 (2007).
37. Tashiro, A., Makino, H. & Gage, F.H. Experience-specific functional modification of the dentate gyrus through adult neurogenesis: a critical period during an immature stage. *J. Neurosci.* **27**, 3252–3259 (2007).
38. Gass, P., Katsura, K., Zuschratter, W., Siesjö, B. & Kiessling, M. Hypoglycemia-elicited immediately early gene expression in neurons and glia of the hippocampus: novel patterns of FOS, JUN and KROX expression following excitotoxic injury. *J. Cereb. Blood Flow Metab.* **15**, 989–1001 (1995).
39. Nag, S. Cold-injury of the cerebral cortex: immunolocalization of cellular proteins and blood-brain barrier permeability studies. *J. Neuropathol. Exp. Neurol.* **55**, 880–888 (1996).
40. Lavdas, A.A., Grigoriou, M., Pachnis, V. & Parnavelas, J.G. The medial ganglionic eminence gives rise to a population of early neurons in the developing cerebral cortex. *J. Neurosci.* **19**, 7881–7888 (1999).
41. Zecevic, N. & Rakic, P. Development of layer I neurons in the primate cerebral cortex. *J. Neurosci.* **21**, 5607–5619 (2001).
42. Jiménez, D., Rivera, R., López-Mascaraque, L. & De Carlos, J.A. Origin of the cortical layer I in rodents. *Dev. Neurosci.* **25**, 105–115 (2003).
43. Marín, O. & Rubenstein, J.L.R. Cell migration in the forebrain. *Annu. Rev. Neurosci.* **26**, 441–483 (2003).
44. Nery, S., Corbin, J.G. & Fishell, G. Dlx2 progenitor migration in wild type and *Nkx2.1* mutant telencephalon. *Cereb. Cortex* **13**, 895–903 (2003).
45. Adams, R.D. & Victor, M. *Principles of Neurology* (McGraw-Hill, New York, 1977).
46. Tallent, M.K. & Siggins, G.R. Somatostatin acts in CA1 and CA3 to reduce hippocampal epileptiform activity. *J. Neurophysiol.* **81**, 1626–1635 (1999).
47. Richichi, C. *et al.* Anticonvulsant and antiepileptogenic effects mediated by adeno-associated virus vector neuropeptide Y expression in the rat hippocampus. *J. Neurosci.* **24**, 3051–3059 (2004).

ONLINE METHODS

The experiments were conducted in accordance with both the Committee for Animal Care and Use of the Graduate School of Medicine at Kyoto University and the Committee of the National Institute of Neuroscience. All efforts were made to minimize animal suffering and the number of animals used.

Retrovirus-mediated GFP labeling of newly generated neurons. To visualize the detailed morphology of progenitor and newly generated cells, we used a modified form of GFP, which had with a membrane targeting signal derived from the N-terminal SH4 region of the Src family kinase Fyn²⁷ at the 5' end. At the 3' end, the modified GFP contained the woodchuck hepatitis virus post-transcriptional regulatory element (WPRE, a gift from T.J. Hope, Northwestern University) to improve expression by modification of RNA polyadenylation, RNA export and/or RNA translation.

The retrovirus vector was derived from murine leukemia virus. To construct the pDON-AI-CMV-Fyn-GFP-WPRE retrovirus, we cut the pDON-AI plasmid (Takara Bio) with *Bam*HI and blunted it. The pBS-CMV-Fyn-GFP-WPRE construct was digested with *Xba*I and the resulting fragment CMV-Fyn-GFP-WPRE was inserted into the linearized pDON-AI. To construct the pDON-5-SYN I-Fyn-GFP-WPRE retrovirus, we digested the pENT-CMV-Fyn-GFP-WPRE construct with *Hind*III and *Eco*RI. The resulting Fyn-GFP was inserted into the same site of pBS-SYN I-WPRE. First, pBS-SYN I-Fyn-GFP-WPRE was digested by *Xho*I and blunted. Second, pBS-SYN I-Fyn-GFP-WPRE was sequentially cut with *Not*I. The pDON-5 plasmid (Takara Bio) was cut by *Pma*CI and *Not*I. The resulting fragment SYN I-Fyn-GFP-WPRE was then inserted into the linearized pDON-5. The retrovirus was produced according to the manufacturer's instructions accompanying the retrovirus packaging kit (Takara Bio). The resulting viral particles in the culture supernatant were collected and adjusted to 1.0×10^6 transducing units per ml.

Adult Wistar rats (6-month-old males, 450–550 g body weight; for L1-INP cell analysis, 10 rats; for ischemic analysis of L1-INP cells, 8 control and 8 ischemic rats at 4 d and at 1 week after ischemia, total 32 rats; for characterization of postmitotic cells, 6–15 control and 6–15 ischemic rats at each time period, total 72 rats; for c-Fos expression analysis, 6 control and 6 ischemic rats at 4 weeks after ischemia, total 12 rats) were deeply anesthetized with chloral hydrate (35 mg per 100 g of body weight). The virus ($0.2 \mu\text{l}$ of 1.0×10^6 transducing units per ml) was stereotaxically injected by pressure through a glass micropipette attached to Picospritzer III (General Valve) into the rat somatosensory cortex of both hemispheres (2.0–3.5 mm posterior to bregma, 3.5–5.0 mm lateral and 0.2 mm depth below the cortical surface). A tip of the glass micropipette (tip diameter $\leq 40 \mu\text{m}$) was cut to 40 degrees to smoothly prick the cortex (**Supplementary Fig. 5**). One hemisphere received a total of $3.2 \mu\text{l}$ (16 injection sites in $1.5 \text{ mm} \times 1.5 \text{ mm}$ square) of the virus solution or Hoechst 33258 ($1 \mu\text{g ml}^{-1}$). Ischemia was induced as described previously⁴⁸. Briefly, 2 d after the injection, both common carotid arteries were transiently occluded with clamps for 10 min. Control animals were treated identically, except for occlusion of common carotid arteries. The rats were allowed to survive for 1, 2, 4 and 8 weeks after ischemia and were then killed by perfusion.

Antibodies. For primary antibodies, we used mouse monoclonal antibodies to calbindin (1:2,000, Sigma), calretinin (1:10,000, Chemicon), CD11b (clone OX-42, 1:100, BMA Biomedicals AG), CD34 (1:1,000, Santa Cruz Biotechnology), GAD65/67 (1:2,000, Enzo Life Sciences International), GAD67 (1:10,000, Chemicon International), GFAP (1:1,000, Sigma), GFP (1:1,000, Molecular Probes), Ki67 (1:10, Zymed), NeuN (1:200, Chemicon International), NG2 (1:400, Chemicon International), oligodendrocytes (clone CE-1, 1:2,000, Chemicon International), panNa_v (1:1,000, Sigma), parvalbumin (1:2,000, Sigma), pH3 (1:200, Upstate Biotechnology), proteolipid protein (1:1,000,

Chemicon International), PSA-NCAM (clone 2-2B, IgM, 1:1000, Chemicon International) and S100 β (1:1,000, Sigma), rat monoclonal antibody to BrdU (1:100, Abcam), rabbit polyclonal antibodies to c-Fos (1:5,000, Abcam), ChAT (1:500, Chemicon International), GABA (1:1,000, Sigma), GFP ($1 \mu\text{g ml}^{-1}$), Ki67 (1:10, Ylem), MafB (1:200, Bethyl Laboratories), MAP2 (1:1,000, Chemicon), Na_v1.6 (1:100, Alomone Labs), Nkx2.1 (1:800, Santa Cruz Biotechnology), NPY (1:2,000, Sigma) and SOM (1:2,000, Peninsula), guinea pig antibody to GFP ($1 \mu\text{g ml}^{-1}$), and goat polyclonal antibody to Ki67 (1:50, Santa Cruz Biotechnology). For secondary antibodies, we used antibody to mouse IgG Cy3 (1:200, Chemicon International), antibody to mouse IgG Alexa 405 (1:200, Molecular Probes), antibody to mouse IgG Alexa 488 (1:200, Molecular Probes), antibody to mouse IgM Cy3 (1:200, Chemicon International), antibody to rat IgG Alexa 594 (1:200, Molecular Probes), antibody to rabbit IgG Alexa 350 (1:200, Molecular Probes), antibody to rabbit IgG Alexa 488 (1:200, Molecular Probes), antibody to rabbit IgG Alexa 594 (1:200, Molecular Probes), antibody to rabbit IgG Alexa 647 (1:200, Molecular Probes), antibody to guinea pig IgG Alexa 488 (1:200, Molecular Probes), antibody to guinea pig IgG Alexa 594 (1:200, Molecular Probes) and antibody to goat IgG Alexa 488 (1:200, Molecular Probes).

Immunofluorescent analysis. Adult male Wistar rats were used as described above. Fixation and immunofluorescent staining were performed as described previously⁴⁹. For the analysis with BrdU, rats were intraperitoneally subjected to a single injection of BrdU (50 mg per kg) each day for 5 d. At 24 h after the last injection, the rats were deeply anesthetized with sodium pentobarbital (50 mg per kg) and killed by perfusion with 4% formaldehyde in 0.1 M phosphate buffer (wt/vol, pH 7.2). Hoechst 33258 (Sigma) was used to stain nuclei. We took double-staining images in sequential mode using a confocal microscope (TCS SP2, Leica). The confocal laser-scanning images were taken as a z stack with an optical slice thickness of 120 nm (pinhole corresponding to 1 Airy unit) using a $10\times$ objective lens (HC PL APO, NA = 0.40, Leica), a $20\times$ lens (N PLAN, NA = 0.40, Leica) and a $63\times$ lens (HCX PL APO, NA = 1.40, Leica).

To count the numbers of GFP-positive or Ki67-positive cells in the brains, we coronally and sequentially cut brain sections at $35\text{-}\mu\text{m}$ section thickness from the olfactory bulb to the posterior region of midbrain. After all sections were co-stained with the indicated antibodies, the total numbers of GFP-positive or Ki67-positive cells in all of the sections were counted.

Environmental enrichment. An enriched environment was made according to a previous report⁵⁰. Briefly, when not housed in the enriched cages, one rat was housed in a standard cage (length \times width \times height, $25 \times 35 \times 15 \text{ cm}$). In the enrichment study, three rats were housed together for 2 h in an enriched cage, which was a large cage (length \times width \times height, $50 \times 60 \times 60 \text{ cm}$) with three tunnels, one ladder and one running wheel, and sawdust was spread over the floor of the cage along with some kinds of nuts.

Statistical analysis. Data were analyzed by paired Student's *t* test or by one- or two-way ANOVA, and then by Tukey *post hoc* test. Error bars represent s.d.

48. Sairanen, T.R., Lindsberg, P.J., Brenner, M., Carpen, O. & Sirén, A.-L. Differential cellular expression of tumor necrosis factor- α and type I tumor necrosis factor receptor after transient global forebrain ischemia. *J. Neurol. Sci.* **186**, 87–99 (2001).

49. Ohira, K. *et al.* A truncated tropo-myosin-related kinase B receptor, T1, regulates glial cell morphology via Rho GDP dissociation inhibitor 1. *J. Neurosci.* **25**, 1343–1353 (2005).

50. Kempermann, G., Kuhn, H.G. & Gage, F.H. More hippocampal neurons in adult mice living in an enriched environment. *Nature* **386**, 493–495 (1997).

Copyright of Nature Neuroscience is the property of Nature Publishing Group and its content may not be copied or emailed to multiple sites or posted to a listserv without the copyright holder's express written permission. However, users may print, download, or email articles for individual use.